PCCP

Self-organisation of inorganic elements on Si(001) mediated by pre-adsorbed organic molecule.

SCHOLARONE™
Manuscripts

ARTICLE

Self-organisation of inorganic elements on Si(001) mediated by pre-adsorbed organic molecule

A. Racis[*a], L.Jurczyszyn[a], M. Bazarnik[bc], W. Koczorowski[b], A. Wykrota[b], R. Czajka[b], M.W. Radny[bd]

Combined theoretical and experimental study on the adsorption of an isolated benzonitrile molecule on the Si(001) surface, followed by the adsorption of Al (group III), Pb (carbon group) and Ag (transition metal) is presented. It is shown that two new adsorption sites with enhanced reactivity are formed on the surface in the vicinity of the pre-adsorbed molecule. This is evidenced by the increase of the calculated binding energy of the metallic ad-atoms adsorbed at these sites. Experimentally, this enhanced local reactivity of the modified surface is only partially retained when more metallic atoms are adsorbed on the modified surface at room temperature. This is evidenced by the formation of 1-dimensional atomic chains (Pb, Al) attached to one side of the pre-adsorbed molecule.

I. Introduction

Interactions of metallic elements with semiconductor surfaces have been of great fundamental and practical interest for decades [1-15]. Recent, renewed interest in interactions of organic molecules with semiconductor surfaces, especially Si(001), is of enormous importance in attempts to develop functional, atomic-molecular-scale systems for future nano-scaled technologies [16-24,42]. In this paper we study the reaction mechanism of an isolated organic molecule with Si(001) and subsequent reaction with adsorbed metallic elements. Such semiconductor/organic/metal hybrid systems are of primary importance for developing fundamental understanding of the controlled reactivity of Si(001) for its effective organic/metallic functionalisation. It was shown

experimentally and theoretically that diffusing group III-IV elements on the Si(001) surface at room temperature (RT) can be effectively stabilized by surface defects such as C-defects [10,11,13,25,26,27]. It was also shown that this process leads to the formation of stable atomic-wide chain-like structures pinned to the defect. Interestingly, the other, commonly observed defects on Si(001), such as A and B defects, have not been observed to act as nucleation centers for diffusing ad-atoms [28]. As a C-defect originates from the dissociation of an adsorbed water molecule [30-34], it has been concluded that the adsorption of some selected molecules on Si(001) may also lead to the local, chemical activation of the surface. Indeed, a recent study has shown that a benzonitrile molecule after adsorption on Si(001) acts as a nucleation centre for the In ad-atoms diffusing on the surface at RT and leads to the formation of the atomic chains pinned to the adsorbed molecule, similarly to the C-defect [40]. Also, a new stable configuration of a benzene molecule chemisorbed on Si(001)

[a.] Institute of Experimental Physics, University of Wrocław, Plac Maksa Borna 9, 50-204 Wrocław, Poland
[b.] Institute of Physics, Poznań University of Technology, Piotrowo 3, 60-965 Poznań, Poland
[c.] Department of Physics University of Hamburg, Jungiusstrasse 11, D-20355 Hamburg, Germany
[d.] School of Mathematical and Physical Sciences, The University of Newcastle, Callaghan 2308, Australia
[*] Corresponding author: agar@ifd.uni.wroc.pl

reported recently, has been shown to be formed in the vicinity the C-defect [29].

In this contribution we investigate the effect of benzonitrile molecule adsorbed on the Si(001) on the subsequent reaction and aggregation of different types of metallic adsorbates such Al (group III metals), Pb (carbon group) and Ag (transition metal). Our theoretical studies were also partially supplemented by STM measurements, i.e. were limited to isolated molecule on Si(001) and subsequent reaction with the Al and Pb ad-atoms. We show that upon molecular adsorption the modified Si(001) substrate becomes locally, chemically activated and that the subsequent reaction of the metallic elements leads to their adsorption in the vicinity of the adsorbed molecule. We also show that the predicted enhanced reactivity of the modified surface will only be partially retained when metallic atoms are adsorbed on the modified surface at room temperature. The study reveals the mechanism that is responsible for the modification of the chemical reactivity of Si(001) and verifies that the molecules on Si(001), similarly to the C-defect, can lead to spontaneous, controlled organization of various metallic elements on this technologically important substrate.

II. Methodology

Computational. Total energy and electronic structure calculations were performed using the DFT method as implemented in the Fireball code [35-38]. The local orbital pseudo-atomic basis set was used along with the pseudopotentials for the ion cores and the electronic exchange-correlation contributions within the local-density-approximation (LDA) functional of Ceperly and Alder [39]. The calculated bulk Si lattice constant of 5.46 Å was used to construct the six layer asymmetric slab to model the Si(001)-c(4x2) reconstructed surface within the large (8x6) surface unit cell. The dangling bonds at the bottom of the slab were saturated by hydrogen atoms. In the total energy calculations the benzonitrile molecule, metallic ad-atoms and the four topmost atomic layers of the substrate were allowed to relax. The adsorption energies were calculated using the following formula:

$$E_{ads} = -[E_{m+s} - (E_m + E_s)]$$

where E_{m+s} represents the calculated total energy of the system composed of the substrate and the adsorbate molecule or ad-atom), E_s denotes the total energy of the clean substrate, and E_m is the energy of a free (gas phase) molecule or ad-atom.

To estimate the kinetics effects on the diffusing ad-atoms on the modified Si(001) surface we have calculated the activation energies (barriers) for selected diffusion pathways using the Nudged Elastic Band (NEB) method [44] implemented in the Fireball code. The activation energies were used to calculate the inverse of the Arrhenius rate [combined with a typical for the Si(001) surface attempt frequency ($\sim 10^{12}$ Hz) and the temperature at which the experimental data were collected (room temperature, T=300K)], to obtain the time scale of the corresponding diffusion processes.

The electronic properties have been analyzed based on the calculated local density of states (LDOS) distributions. In Fireball, the energy eigenvalues are determined via the corresponding Green function matrix which is also used to construct the density of the states (DOS) of the whole system. This *total* DOS contains information about the *local* DOS (LDOS) associated with each valence orbital of each atom in

the system. The local orbital pseudo-atomic basis set allows LDOS to be extracted from the *total* DOS by projecting the latter on selected valence orbitals of an selected atom. For a group of atoms selected from the whole system the corresponding LDOS distribution is calculated as a sum of the LDOS contributions from the valence orbitals of each atom within the selected group.

The electronic structure analysis based on LDOS is supplemented by the charge density distributions calculated for the electronic states associated with the characteristic LDOS features.

Experimental. The room temperature (RT) scanning tunneling microscopy (STM) experiments were carried out in an ultra-high vacuum (UHV) system with a base pressure in the 10^{-11} mbar regime. The As-doped Si(001) sample were outgassed at 970 K and subsequently flashed at 1600 K. Benzonitrile molecules were dosed out of a saturated vapors into a separate chamber using a home-built evaporator [43]. The cleanness of the molecule vapor was checked by mass spectrometry prior exposition. The samples were exposed to a partial pressure of $4*10^{-10}$ mbar of benzonitrile for 5' resulting in a coverage of approximately 0.05 monolayer (ML). The Al and Pb were deposited by means of electron bombardment of pieces of bar (for Al purity of 99.97%, for Pb purity of 99.9998%) out of a Mo crucible at a base pressure of $<1 \times 10^{-10}$ mbar and a flux of 0.5 ML min^{-1} in a direct line of sight onto the Si substrate at room temperature. Tungsten sputtered tips were used in all STM measurements.

III. Results

A. A single benzonitrile molecule on Si(001).

i) Experimental STM images and structure assignment.

The RT STM filled and empty states images of an isolated benzonitrile molecule (C_6H_5CN) adsorbed on Si(001) are shown in Figs.1a and 1b, respectively. In the occupied states image of Fig.1a, the adsorbed molecule appears as a protrusion above two silicon dimers located on the two adjacent dimer rows. The feature on one row is associated with the carbon ring, and a very discreet protrusion on the neighboring dimers row is associated with nitrile (-CN) group. Close inspection of the filled state STM images of Figs.1a and 1c also shows that the adsorbed molecule pin the flipping, bare Si dimers in close proximity of the adsorption site in the local c(4x2) and p(2x2) reconstructions. In the empty states image (Fig.1b) the adsorbed molecule appears as a one bright protrusion (due to carbon ring) and two much smaller features on the opposite side of the nitrile group. Figure 1c shows the enlarged filled state image of the adsorbed molecule with the calculated bonding configuration of the adsorbate. The results presented in Figs.1a-1c are entirely consistent with that reported in [40]. Also, our experimental STM data and that presented in Ref. [40] clearly show that the adsorbed molecule is immobile on the surface at room temperature.

The calculated most stable geometry of the isolated benzonitrile molecule adsorbed on the clean Si(001)-c(4x2) reconstructed surface, with the calculated binding energy of 2.59 eV, is shown in Fig.2. The structural details are presented in Table I. The data shows that the phenyl ring of the molecule interacts with two adjacent silicon dimers on the same dimer row (C1-Si4 and C4-Si2 in Fig.2), while the nitrile functional group interacts with one dimer on the neighboring silicon dimer row (N-Si7 in Fig.2). This dimer-row bridge configuration, with the molecule adsorbed between two

adjacent dimer rows, also pins the bare Si dimers on each affected dimer row, as evidenced by the experimental filled state STM images of Figs.1a and 1c.

The stability of the dimer-row bridge configuration is due mainly to two covalent bonds formed between the phenyl ring and the substrate Si dimer atoms. The formation of these bonds breaks, however, two intra-dimer π-bonds in the Si dimers interacting directly with the molecule (dimers c, d in Fig.2a). This is evidenced by the calculated structural data - the bond lengths of the chemisorbed Si dimers increase and their buckling angle decreases with respect to the bare silicon dimers (see Table I) – bonds being broken and two unsaturated, unpaired dangling bonds are formed on the Si atoms at the free ends of the chemisorbed dimers. They can be identified in the experimental STM images as protrusions indicated by letter A in Figs.1a and 1c.

The interaction of the substrate with the molecule via the nitrile group can be realized in two ways - the N atom of the group is attached to an up-Si dimer atom or to a down-Si dimer atom. In both cases the newly formed N-Si bond breaks the intra-dimer π-bond and the unpaired dangling bond is formed at the free end of the chemisorbed dimer (protrusion indicated by letter B is the STM image of Figs.1a and 1c). We have found, however, that the configuration where the N atom bonds to the down-Si dimer atom is energetically by 0.36 eV more favourable. The most stable structure is shown in Fig.2, and it is the only one considered later in this study.

The STM manipulations performed on the adsorbed molecule, as reported in [40], indicate that the adsorption of benzonitrile is non-dissociative. Also the adsorbed molecule is expected to remain structurally similar to its gas phase geometry. Close inspection of the calculated structural data shows, however, that the interaction of the molecule with Si(001) breaks the aromatic structure of the phenyl ring and two spatially localized, double bonds (C5-C6 (7) and C3-C2 (4) in Fig.2) are formed with the bond lengths of 1.32-1.35 Å. The data also shows that length of the C-N bond in the free molecule and after its adsorption is very similar: 1.19 Å and 1.22 Å, respectively, indicating that the bond within the nitrile group in the gas phase is only slightly affected by the formation of the new bond between the Si and N atoms.

ii) Electronic structure.

Further insight into the bonding structure of the adsorbed system is given by the analysis of the electronic local density of states (LDOS) projected on the adsorbed molecule. The calculated LDOS distribution is shown in Fig.3 – it was obtained as a sum of the LDOS contributions associated with the valence orbitals of all atoms of the molecule. Features (a) and (b) of Fig.3 located ~1.8 eV and ~4.6 eV below the Fermi level, respectively, are both composed of the p_z states of the C1 and C4 ring atoms and the p_z states of the Si4 and Si2 substrate atoms (see Fig.2). The interaction between these states leads to the formation of the C1-Si4 and C4-Si2 (phenyl ring-substrate) covalent bonds. In addition, feature (a) also consists of the p_z states of the C5 and C6 ring atoms, while feature (b) contains the p_z states of the C5 andC6 as well as C2 and C3 ring atoms. As a result both (a) and (b) features also represent two C5=C6 and C2=C3 double bonds formed on the phenyl ring upon adsorption. The partial charge distributions calculated for the electronic states contributing to features (a) and (b) are presented in Figs.4 a) and 4 b), respectively.

Peaks (c) and (d) in LDOS of Fig.3 consist mainly of the p_x and p_y states of the phenyl ring atoms and as such describe the bonding structure within the ring. Peak (i) as well as peaks (g), (h) and (l), describes the bonding between the ring C atoms and the ring hydrogen atoms, as well as the bonding within the nitrile group, respectively.

Figures 4 c), 4 d), 4 e) and 4 f) show the partial charge distributions associated with LDOS features (e), (f), (j) and (k) shown in Fig.3. All of them are related to the bonds in which the N atom of the nitrile group is involved. Features (e) and (f) represent the formation of the σ and double (π) bonds, respectively, within the nitrile group, while peaks (j) and (k) describe bonding between the N atom and the Si substrate atoms. The latter originates predominantly from the contributions of the p_x states of the N atom and the s state of the down-Si dimer atom.

The revealed energetic order of the various bonds formed in the adsorbed system explains some of the experimental results shown in Fig.1 and reported in [40]. Firstly, as the C-N bond is significantly lower in energy then the C=C double bonds, only the latter should be imaged in the filled state STM images. This agrees with the experimental STM images of Fig.1, where the large white protrusion indicated by symbol C can be identified as a feature associated with the C=C double bonds on the phenyl ring. Secondly, the calculations also show that while the molecule is bonded to the substrate via two C-Si bonds and one N-Si bond, the latter is much lower in energy and therefore much stronger. Moreover, the bonds within the adsorbed molecule, especially within the nitrile group, are just slightly weaker then the Si-N bond. Such energetics order explains the results of direct manipulation of the adsorbed

molecule using the STM tip reported in [40]. As it was demonstrated in [40] increasing the bias voltage and keeping simultaneously the tip-sample separation constant leads to the rotation of the adsorbed molecule by ~50 deg around the strong N-Si bond, which remains preserved during rotation. Such transformation of the molecule is possible because weaker Si-C bonds are broken during rotation and are restored in the new configuration of the adsorbed molecule.

One of the main goals of this study is to understand the role of the unpaired Si dangling bonds that appear on the three silicon dimers upon adsorption, play in changing locally the chemical properties of the Si(001) substrate. To clarify this point the local density of states (LDOS) projected on the three silicon atoms located at the free ends of the chemisorbed dimers (c, d and b in Fig.2) that are presented in Fig.5 will be discussed next.

Figure 5a shows LDOS associated with the free ends of dimers c and d affected by the chemisorbed ring (atoms Si1 and Si3, respectively, in Fig.2). The sharp LDOS peak in Fig.5a, located 0.2 eV below the Fermi level, represents the two dangling bonds that are localized at the free ends of the chemisorbed dimers. This LDOS feature is composed almost solely of the p_z orbitals associated with the Si1 and Si3 atoms indicating that the intra-dimer -bond on these chemisorbed dimers is broken. However, the side overlapping along the dimer row of the p_z orbitals, that are located on the adjacent atoms S1 and Si3, leads to the appearance of the inter-dimer -interaction and inter-dimer -bond. It is the latter that is characterized by the LDOS peak at 0.2 eV in Fig.5a. The charge density plot associated with this peak is shown in Fig.5d and illustrates the charge transfer within the intra-dimer -bond.

LDOS related to the free end of dimer b affected by the nitrile group (atom Si8 in Fig.2) is presented in Fig.5b. This figure also shows LDOS projected on the Si down-atom on un-chemisorbed dimer a (atom Si6) adjacent to dimer b. Finally, for comparison LDOS associated with two Si atoms of a bare Si dimer on Si(001) is shown in Fig.5c. We observe that by contrast to LDOS of Fig.5a, LDOS of Fig.5b is very similar to that for the bare Si dimer, suggesting a negligible effect of a broken, single, intra-dimer π-bond on the LDOS distribution (compare Figs.5b and 5c).

B. Functionalisation of the modified Si(001) surface.

i) Computational study.

It was demonstrated that diffusing In ad-atoms on Si(001) with preadsorbed benzonitrile can be stabilized and aggregated in the form of the chain-like structures [40]. The latter was shown to be initiated by the adsorption of the In atom between two dangling bonds on two Si dimers directly interacting with the phenyl ring of the adsorbed molecule. In the present contribution we investigate the adsorption mechanism of transition metal element (Ag) and an element from carbon group (Pb) on the modified Si(001) substrate. The reaction of Al (group III) is also investigated to provide a link to the published data for the In/Molecule/Si(001) system [40].

The interactions of the ad-atoms with the substrate are examined at two adsorption sites on modified Si(001) identified in the previous section as "reactive" - (i) between two dangling bonds on two Si dimers directly interacting with the phenyl ring of the adsorbed molecule (Configuration A) and, (ii) in the vicinity of the single dangling bond on the Si dimer interacting with the nitrile group (Configuration B). The latter case was not considered before.

The relaxed atomic structures for the Al, Pb and Ag ad-atoms in both Configuration A and Configuration B are shown schematically in Fig.6. Table II contains the calculated adsorption energies of the ad-atoms in both configurations as well as the characteristic inter-atomic distances and angles in the most stable geometries.

We observe that for the Al and Pb ad-atoms the adsorption geometries in Configurations A and B are very similar (see Figs.6a and 6b). In Configuration A these ad-atoms adsorb at the bridge sites between two dangling bonds on two adjacent Si dimers on the same dimer row directly interacting with the phenyl ring of the adsorbed molecule, while in Configuration B between the single dangling bond on the Si dimer interacting with the nitrile group and the adjacent bare Si dimer on the same dimer row. By contrast, for the Ag ad-atom we have found several different adsorption structures as derivatives of Configurations A and B. The two most stable are presented on Fig.6c as structures (i) and (ii). We have found that structure (ii) is by 0.29 eV (Configuration A) and 0.4 eV (Configuration B) energetically more favourable than structure (i). Also, in contrast to the stable structures induced by the Al and Pb ad-atoms, in the most stable structure (ii) the Ag ad-atom interacts with two substrate atoms on adjacent dimer rows - Si12 and Si3 (Configuration A) and Si8 and Si15 (Configuration B). Similar ad-atom geometries and energetic preferences were found for a single Ag ad-atom adsorbed on clean Si(001) [41].

The data in Table II shows that the ad-atom adsorption energies in Configurations A are by 0.62 eV (Al), 0.96 eV (Pb) and 0.64 eV [Ag, structure (ii)] higher than those on the clean Si(001) surface. We also observe that while the ad-atom

binding energies in Configuration B are also higher than that on the clean surface - by 0.12 eV (Al), 0.21 eV (Pb), and 0.47 eV [Ag, structure (ii)] - they are considerable lower than in Configuration A. For the Al and Pb ad-atoms this difference arises because in Configuration A the ad-atoms interact with two unsaturated, chemically active dangling bonds at the free ends of two chemisorbed Si dimers, while in Configuration B the ad-atoms interact only with one unsaturated dangling bond. The considerable smaller difference between the binding energies of the Ag ad-atom in Configurations A and B can be explained by the fact that in both configurations Ag interacts with only one unsaturated Si dangling bond (see Fig.6c, structure (ii)).

The enhanced local chemical activity of the modified Si(001) substrate, measured by comparing the binding energies the adsorbed ad-atoms on clean and modified Si(001), can initiate the process of one-dimensional aggregation of the ad-atoms, if more of them adsorb on the surface [1,2,9,10]. The stable geometries of these aggregates are expected to be the same as those reported earlier, i.e, 1-D atomic chains formed across the Si dimer rows [1,2]. It should be noted, however, that for the Ag ad-atoms, despite the enhanced local chemical activity of the substrate, the ad-atom adsorption geometries do not provide any new active sites for subsequent ad-atom adsorption and the formation of the 1D ad-atomic chain will not occur [12]. Therefore in the subsequent sections, the interaction of the ad-atoms with the substrate in the vicinity of the pre-adsorbed molecule will be analyzed further for the Al and Pb ad-atoms only.

To estimate the kinetics effects on diffusing ad-atoms on the modified Si(001) surface we have calculated the activation energies (barriers) and the time scale of the corresponding diffusion processes of the Pb adatom in Configurations A and B.

In Configuration A the anchoring site generated on Si(001) by the adsorbed molecule is located in the front of the molecular carbon ring. We have analysed three competing diffusion pathways taken by the Pb adatom during detachment, i.e, the transition of the adatom from the anchoring site to the sites between the clean Si dimers on the adjacent dimer row (Pathway 1), and on the same dimer row (Pathway 2 and Pathway 3). The corresponding reverse processes (attachment of the Pb adatom) were also studied.

The energy barrier associated with Pathway 1, i.e., the shift of the Pb ad-atom from the anchoring site to the next nearest adsorption site across the dimer row (detachment) was calculated to be 1.02 eV, while the ad-atom movement in opposite direction (attachment) requires the activation energy of 0.16 eV. The latter barrier is very small and rapidly crossed at room temperature - the estimated timescale for this process is of the order of 0.5ns at room temperature. As the estimated timescale for the detachment process is 38h at room temperature (activation energy of 1.02 eV), it is clear that following Pathway 1 the Pb adatom will immediately be adsorbed at the anchoring site near the molecule.

The activation energy of 1.16 eV was obtained for the detachment of the ad-atom to the nearest adsorption site along the direction parallel to the dimer row towards atom Si3 (Pathway 2, see Fig.6). The movement in opposite direction (attachment) requires activation energy of 0.52 eV. The corresponding timescales for these processes at room temperature are estimated to be 8500h and 0.5ms,

respectively. This is similar to Pathway 1 and from the two processes described by Pathway 2 only the attachment of the Pb adatom to the adsorption site near the molecule will lead to the stable adatom configuration.

The activation energy of 1.90 eV was calculated for the detachment of the ad-atom to the nearest adsorption site along the direction parallel to the dimer row towards atom Si1 (Pathway 3, see Fig.6). The shift in opposite direction (attachment) requires activation energy of 1.10 eV. The corresponding timescale for these processes at room temperature are estimated to be $2.3*10^{16}$h and 840h, respectively. Clearly, none of these barriers would be accessible at room temperature. In conclusion in Configuration A the diffusing Pb adatom on modified Si(001) at room temperature will be trapped and readily adsorbed at the anchoring site near the molecule.

Similar calculations performed for Configuration B, where the anchoring site is located near the molecular nitrile group, leads to considerably different results. The detachment of the Pb ad-atom from this anchoring site to the nearest adsorption site between the Si dimers across the dimer row is associated with the activation energy of 0.50 eV. The reverse process (attachment) requires the activation energy of 0.36 eV. The estimated timescale for these processes at room temperature are 250μs and 0.5ns, respectively. The latter indicates that there is not much preference for the attachment over detachment processes as both barriers can be readily crossed at room temperatures and both processes are very competitive. Also, as the STM recording time is of the order of minutes, none of these processes can be observed in STM. Similar situation occurs when the Pb adatom is shifted along

the dimer row towards the Si8 atom (see Fig.6) – the activation energies for detachment and attachment of the adatom along this pathway were calculated to be 0.51 eV and 0.27 eV, respectively. By contrast, the activation energies for the shift of the Pb adatom along the dimer row towards atom Si6 (end in opposite direction) were calculated to be 1.54 eV (1.42 eV). Clearly, none of these barriers is accessible at room temperature. In conclusion Configuration B cannot stabilize the diffusing Pb adatom on Si(001) at RT and the ad-atom can only be trapped by the molecule at the adsorption site near Configuration A. Such spatial stabilization of the diffusing ad-atom can initiate the one-dimensional aggregation of other ad-atoms on the Si(100) surface as observed in experiment (see also Refs.[1,2,10]). Analogous behavior was observed for diffusing In adatoms on the modified Si(001) at RT [40] indicating that similar behavior should also be observed for the Al/Si(001) system.

Figure 7a presents the local density of states distributions calculated for the Al ad-atom and two Si substrate atoms that directly interact with the ad-atom in Configuration A. The corresponding data obtained for the Pb ad-atom is shown in Fig.7b.

The data in Fig.7 shows that the system with the Al ad-atoms is metallic (Fig.7a) while the one with the Pb ad-atoms is semiconducting (Fig.7b). Apart from that, the energetic distribution and compositions of the characteristics LDOS features are similar in both cases. Feature (a) is built up by the p_x states of the ad-atom (Al or Pb) and the p_z states associated with the free Si atoms on the two Si dimers chemisorbed by the phenyl ring (Si1 and Si3 in Figs. 6a and 6b). The corresponding charge distributions shown in Figs.8a and 8b,

for the Al and Pb ad-atoms, respectively, demonstrate the antibonding character of this combination of states. Peaks (b) in Figs.7a and 7b are composed of the p_y states of the ad-atom (Al or Pb) and the p_z states of the Si1 and Si3 substrate atoms. As shown in the charge distributions presented in Figs.8c and 8d for the systems with the Al and Pb ad-atoms, respectively, the combination of these states leads to the bond formation between the Al/Pb ad-atoms and the substrate. The LDOS features with lower binding energies are built up by the s/p states of the ad-atom and the Si1 and Si3 atoms, and the features with the lowest energies originate almost solely from the s states associated with the ad-atom and the Si1/Si3 atoms.

The LDOS distributions associated with the Al and Pb ad-atoms, and two Si substrate atoms interacting directly with the ad-atom in Configuration B are shown in Figs.9a and 9b, respectively. The data shows that both systems are semiconducting. Feature (a) in LDOS for the Al-related system (Fig.9a) is composed mainly of the p_y states associated with the ad-atom and the p_z/p_x states of the Si atoms. The corresponding charge distribution is shown in Fig.10a. LDOS maximum (a) for the Pb-related system (Fig.9b) is built up mainly by the p_x states of the Pb ad-atom and the p_z states of the substrate atoms. The related charge distribution is shown in Fig.10b. The data in Figs.10a and 10b indicates on the antibonding nature of these states. This is similar to LDOS features (a) of Figs.7a and 7b. However, as in Configuration B the ad-atoms interact only with one unsaturated Si dangling bond, the bonds between the ad-atoms and the substrate atoms are considerably less symmetric than in Configuration A – compare Fig.10b with Fig.8 b. or Fig.10c with Fig.8c.

LDOS maxima (b) in Figs.9a and 9b are dominated by the p_y states of the ad-atoms (Pb or Al) and the p_z states of the Si substrate atoms. The interaction between these states leads to the formation of two bonds linking the ad-atoms with the Si atoms, as shown in the corresponding charge distributions of Figs.10c and 10d. This is also similar to LDOS features (b) of Figs.7a and 7b (see also Figs.8c and 8d) in Configuration A.

The main contributions to the LDOS features at lower binding energies come from the s states of all of the interacting atoms. The features with lowest energies are composed almost solely of the s states associated with the ad-atom and two substrate atoms, as it was the case in Configuration A.

The calculated electronic structure indicate that in both Configurations A and B, there are ad-atom induced states in the vicinity of the Fermi level that may be active in facilitating the reactions with additional ad-atoms and the formation of 1D atomic chains. However, the calculated energetics suggests that in Configuration B the relative binding energies of 0.12 eV (Al), 0.21 eV (Pb) may be too small to prevent the ad-atoms from diffusing on the surface at room temperature. Our experimental data discussed in the next section confirms this prediction showing that the enhanced reactivity of the modified surface is retained for Configuration A only, as the 1-D chains are formed on one side of the adsorbed molecule.

ii) Experimental studies.

The room temperature STM measurements were performed for the Al and Pb atoms deposited at a very low coverage (lower than 0.1ML) on the Si(001) surface modified by the preadsorbed benzonitrile molecules. In each of the studied cases the 1D atomic chains were observed to grow on the modified surface.

The STM images for the system with Al ad-atoms are shown in Fig. 11. Clearly visible are the Al chains that run across the Si dimer rows. The chains itself have a very low apparent height so the molecule is clearly visible at the end of the chain - see Figs. 11 (c) and (d). The Al chain-like structures pinned to the benzonitrile molecule are also seen in the empty state STM images (see Figs.11 a) and b)). Close inspection of the data indicates that in most of the cases the grow of Al chains takes place at the adsorbed molecule - the number of the Al chains formed on the clean parts of the substrate (i.e. without benzonitrile) is considerably lower. This observation supports our earlier conclusion that preadsorbed benzonitrile increases the local reactivity of the Si(100) substrate and the binding of Al atoms to the substrate in the vicinity of the preadsorbed molecules is much stronger than on clean Si(001). Also the one-dimensional aggregation of the Al ad-atoms takes place only in front of the molecular phenyl ring, as it is shown in Fig.11 d. This indicates that only Configuration A is a precursor for the Al chain growth on the modified Si(001) surface. These results are entirely consistent with the study on the In/Si(001) system [40].

The STM images obtained for the Pb/Si(001) system with the preadsorbed molecules are shown in Fig. 12. Similarly to the Al/Si(001) system, the Pb chains are formed on the surface and run across the Si dimer rows. However, in contrast to the Al chains, the adsorbed molecules have a considerably lower apparent height than the Pb chains so the molecules to which the Pb chains are attached, and the adjacent bare Si dimers, are not clearly visible in the images. The empty state images (see Figs.12d and 12e) clearly show, however, that the formed chains ends by two different protrusions – one is the same as

each segment within the chain while the other is clearly smaller. The presence of the latter indicates that there is a precursor for the Pb chain growth and that the chains growth on one side of the activated site on Si(001). This is similar to the Al/Si(001) system. Based on the results discussed in the previous section we predict that the one-dimensional aggregation of the Pb ad-atoms takes place in front of the molecular phenyl ring, i.e, Configuration A is a precursor for the Pb chain growth on Si(001) modified by the adsorbed benzonitrle.

IV. Summary.

The adsorption of a single benzonitrile molecule and subsequent adsorption of selected metallic elements (Al, Pb and Ag) on the Si(001) surface was studied to clarify the effect of both on the local, chemical activity of the modified substrate.

It is shown that the phenyl ring of the molecule breaks the π bonds on two adjacent Si dimers and two unsaturated Si dangling bonds are formed on the surface. The -CN functional group of the molecule covalently bonds to one Si dimer on the adjacent dimer row and leads to the formation of one additional unsaturated Si dangling bond on the surface. The distribution of these dangling bonds in the vicinity of the adsorbed molecule defines two new active adsorption sites on the modified Si(001) surface.

For the subsequent adsorption of metallic elements on modified Si(001) it is shown that the binding energies of the atomic adsorbates significantly increases when they are located at the new adsorption sites near the adsorbed molecule. This indicates that on modified Si(001), by pre-

adsorbed molecule, the local chemical activity of the substrate is enhanced at these new adsorption sites.

The electronic structures calculated for the Ad-atom/Molecule/Si(001) system for the stable adsorption configurations indicate that in all studied cases there are equally active electronic states near E_F that may facilitate favorable adsorption of additional metallic atoms and formation of 1-D atomic chains on both sides of the adsorbed molecule. However, the total energy calculations show that the adsorption energies of the ad-atoms located near the -CN group of the molecule may be not high enough to prevent the ad-atoms from diffusing on the Si(001) substrate at room temperature. Our experimental results support this prediction. The STM data shows that at room temperature one-dimensional aggregation of diffusing ad-atoms on the surface with the pre-adsorbed molecule occurs only in front of the molecular carbon ring. This means, based on our calculations, that the enhancement of the substrate reactivity in the vicinity of molecular -CN group is too small to stabilize the position of diffusing ad-atoms on the Si(001) surface at room temperature. These results are consistent with the data reported earlier for In/Si(001) with pre-adsorbed benzonitrile [40]. Our results demonstrate that atoms from group III and IV interact with the silicon substrate modified by the adsorbed molecule, in a similar way. By contrast, the co-adsorption of transition metal atoms (Ag) on modified Si(001) was concluded to be different and such that would not lead to the formation of 1D atomic chains.

Acknowledgments

References

1   A. Puchalska, A. Racis. L. Jurczyszyn, M.W. Radny, *Surf. Sci.*, 2013, 608, 188-198.
2   L. Jurczyszyn, M.W. Radny, and P.V. Smith, *Surf. Sci.*, 2011, 605,1881-1888.
3   T.-L.Chan, Y.Y.Ye, C.Z.Wang, and K.M.Ho, *Surf.Sci.*, 2006, 600, L159.
4   T.-L.Chan, C.Z.Wang, Z.-Y.Lu, and K.M.Ho, *Surf.Sci.*, 2003, 524 L694.
5   Z.-C.Dong, D.Fujita, and H.Nejoh, *Phys.Rev.B*, 2001, 63 115402.
6   L.Jure, L.Magaud, P.Mallet, and J.-Y.Veuillen, *Surf.Sci.*, 2001, 482 1343.
7   L.Jure, M.Magaud, J.-M.Gomez-Rodrigez, P.Mallet, and J.-Y.Veuillen, *Phys.Rev.B*, 2000, 61 16902.
8   M.E.Gonzalez-Mendez and N.Takeuchi, *Phys.Rev.B*, 1998, 58 16172.
9   M.W.Radny, P.V.Smith, and L.Jurczyszyn, *Phys.Rev.B*, 2010, 81 085424.
10 P.Kocan, L.Jurczyszyn, P.Sobotik, and I.Ostadal, *Phys.Rev.B*, 2008, 77 113301.
11 P.Kocan, P.Sobotik, I.Ostadal, J.Jaworski, and M.Stevin, *Surf.Sci.*, 2007, 601 4506.
12 P. Kocan, P. Sobotik, I. Ostadal, *Czech. J. Phys.* ,2006, 56 27.
13 M.A.Albao, M.M.R.Evans, L.Nogami, D.Zorn, M.S.Gordon, and J.W.Evans, *Phys.Rev.B*, 2006, 74 037402.
14 L.Magaud, A.Pasturel, L.Jure, P.Magaud, and J.Y. Veuillen, *Surf.Sci.,* 2000, 454 489.
15 N.Takeuchi, *Phys.Rev.B*, 2000, 63 5311.
16 S. F. Bent, *Surf. Sci.*, 2002, 500 879.
17 M. A. Filler and S. F. Bent, Prog. *Surf. Sci.,* 2003, 73 1.
18 R.A. Wolkow, Annu. *Rev. Phys. Chem*, 1999, 50 413.
19 M. Ratner, *Nature (London),* 2005, 435 575.
20 J.A. Barriocanal and D. J. Doren, *J. Am. Chem. Soc.,* 2001, 123 7340.
21 J.T. Yates Jr., *Science*, 1998, 279 335.
22 M.J. Kong, A.V. Teplyakov, J.G. Lyubovitsky, S.F. Bent, *Surf. Sci.*, 1998, 411 286.
23 M.J. Kong, A.V. Teplyakov, J.G. Lyubovitsky, *J. Phys. Chem.,* 2000, 104 3000.
24 F.Tao, S.L.Bernasek, G-Q. Xu, *Chem. Rev.*, 2009, 109 3991.
25 P. Kocan, P. Sobotik, I. Ostadal, *Phys. Rev. B*, 2006, 74 037401.
26 M.A. Albao, M.M.R. Evans, J. Nogami, D. Zorn, M.S. Gordon and J.W. Evans, *Phys. Rev. B*, 2006, 72 037402.
27 B.Pieczyrak, L.Jurczyszyn, *Applied Surf. Sci.*, 2014, 304 91.
28 M.A. Albao, M.M.R. Evans, J. Nogami, D. Zorn, M.S. Gordon and J.W. Evans, *Phys. Rev. B*, 2005, 72 035426.
29 Harikumar K. R.; Polanyi John C.; Zabet-Khosousi Amir, *Surf. Sci.*,2012, 606 1431.
30 M.Z. Hossain, Y. Yamashita, K. Mukai and J. Yoshinobu, *Phys. Rev. B*, 2003, 67 153307.
31 S. Okano, A. Oshiyama, *Surf. Sci.*, 2004, 554 272.
32 J.-Y. Lee, J.-H. Cho, *J. Phys. Chem. B*, 2008, 110 036107.
33 S.-Y. Yu, H. Kim, J.-Y. Koo, *Phys. Rev. Lett.,* 2008, 100 036107.
34 O. Warschkow, S.R. Schofield, N.A. Marks, M.W. Radny, P.V. Smith, and D.R.McKenzie, *Phys. Rev. B*, 2008, 77 201305(R).

35 J.P. Lewis, K.R. Glaesemann, G.A. Voth, J. Fritsch, A.A. Demkov, J. Ortega, and O.F. Sankey, *Phys. Rev. B*, 2001, 64 195103.

36 A.A.Demkov, J.Ortega, O.F.Sankey, M.P.Grumbach, *Phys. Rev. B*, 1995, 52 1618.

37 O.F.Sankey, D,J,Niklewski, *Phys. Rev. B*, 1989, 40 3979.

38 P. Jelinek, H. Wang, J.P. Lewis, O.F. Sankey, and J. Ortega, *Phys. Rev. B,* 2005, 71 235101.

39 D.M.Ceperley, B.J. Adler, *Phys. Rev. Lett.,* 1980, 45 566.

40 D.R. Belcher, M.W. Radny, S.R. Schofield, P.V. Smith, and O. Warschkow, *J. Am. Chem. Soc.,* 2012, 134 15312.

41 K. Kong, H.W. Yeom, D. Ahn, H. Yi, B.D. Yu, *Phys. Rev. B* 67, 235328.

42 M. Bazarnik, L. Jurczyszyn, R. Czajka, K.Morgenstern,   *PCCP*, 2015, 17 5366.

43 A. Wykrota, W. Koczorowski, R. Czajka, *Mater. Sci. Semicond. Process.* , 2014, 17 168.

44 G. Mills, H. Jonsson, G.K. Schenter, *Surf. Sci*., 1995, 324, 305–337
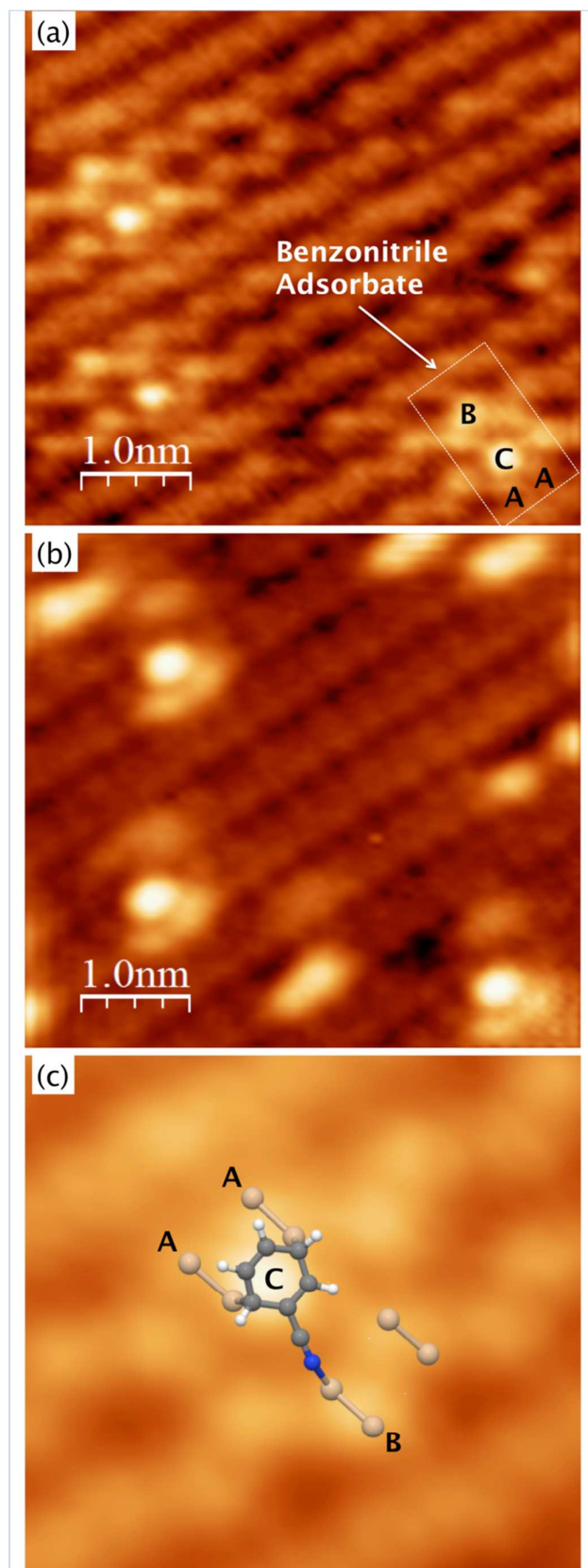
Figure 1. (Colour online) (a) Filled state (U=-2V, It = 100 pA)

and (b) empty state (U=2V, It =120 pA) STM images of the benzonitrile molecule adsorbed on Si(001) at room temperature; (c) a stick-and-ball model of the adsorbed molecule imposed on the filled states STM image (U=-2V, It = 100 pA).
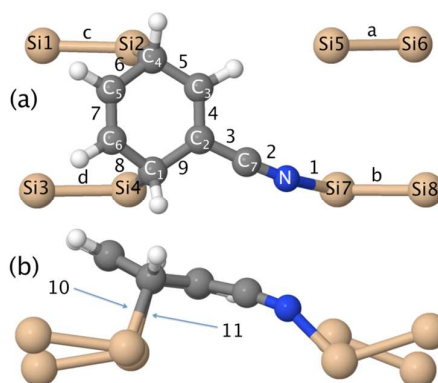
Figure 2. (Colour online) (a) Top and (b) side views of the benzonitrile molecule adsorbed on Si(001) in its most stable configuration. Grey spheres represent the C atoms, blue sphere the N atom, white spheres the H atoms, and brown spheres the Si atoms. Only the first layer atoms of the Si(001)-c(4x2) reconstructed surface are shown.
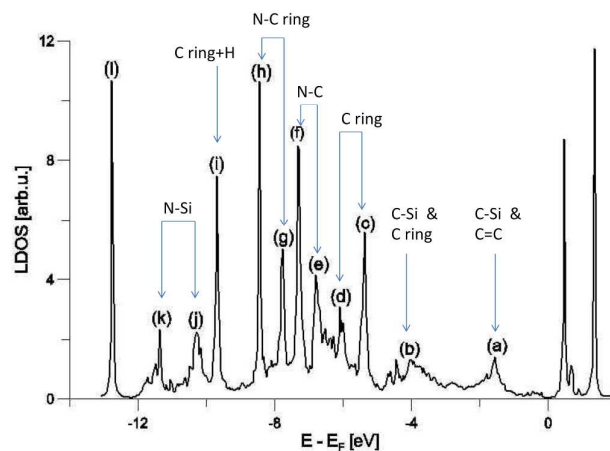
Figure 3. The local density of states (LDOS) distribution calculated of the benzonitrile molecule adsorbed on the Si(001)-c(4x2) surface.

Isosurface values: a) 0.035 e/Å³, b) 0.017 e/Å³, c) 0.041 e/Å³, d) 0.048 e/Å³, e) 0.014 e/Å³, f) 0.035 e/Å³.
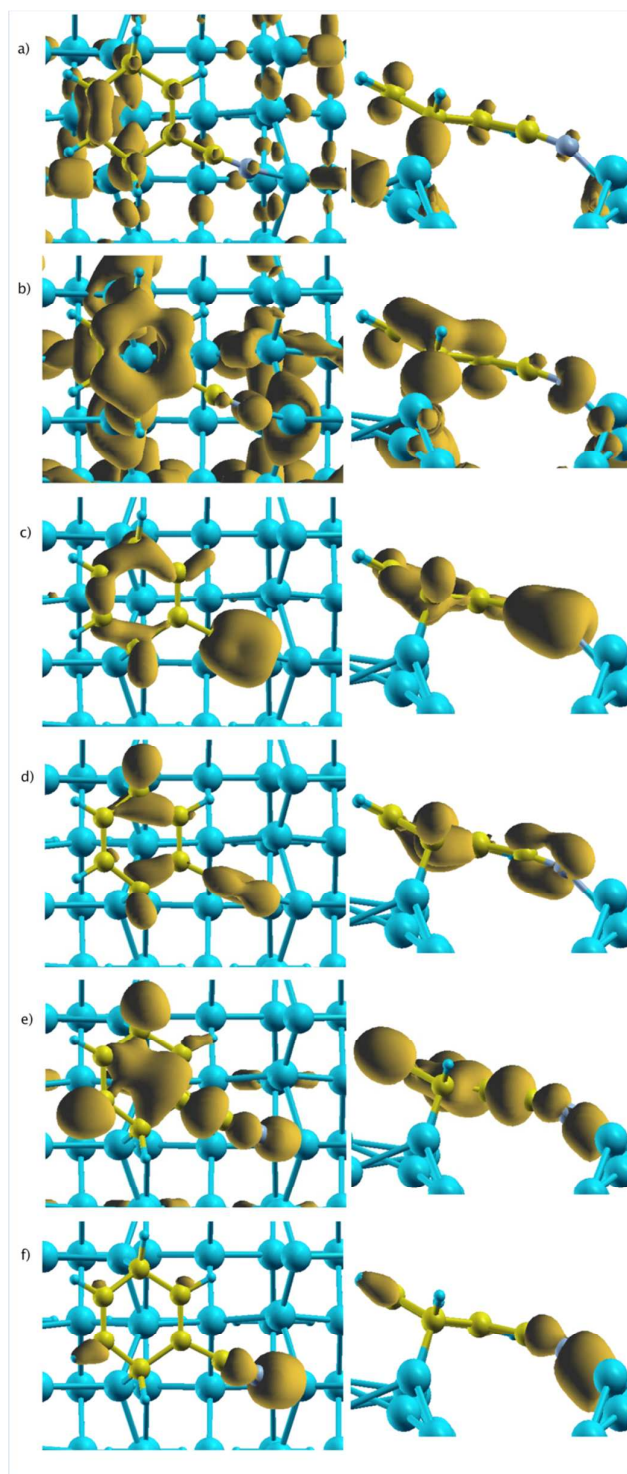
Figure 4. *(Colour online) Charge density distributions of the electronic states associated with the LDOS features (a), (b), (e), (f), (j) and (k) in Fig.3. – a), b), c), d), e), f) respectively. Top and side views of each distribution are presented.*
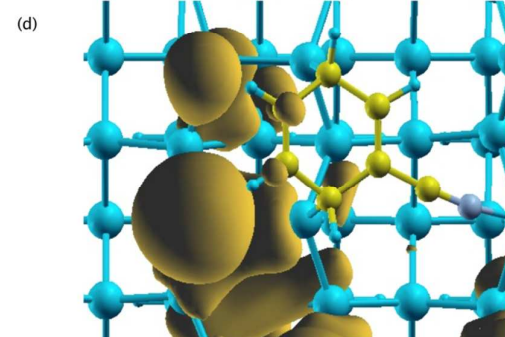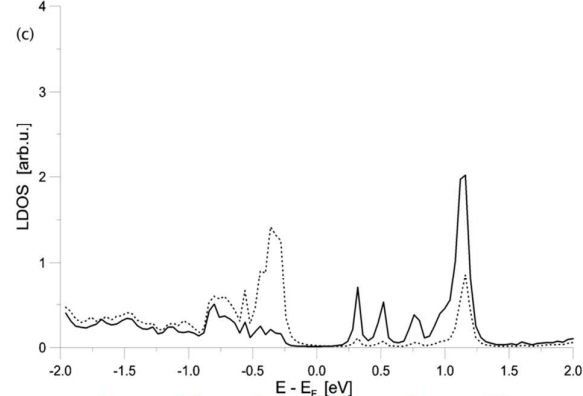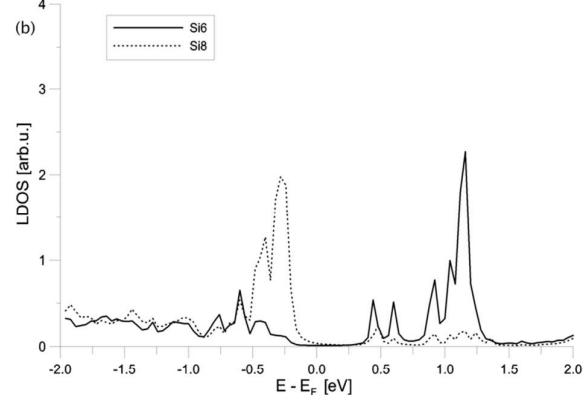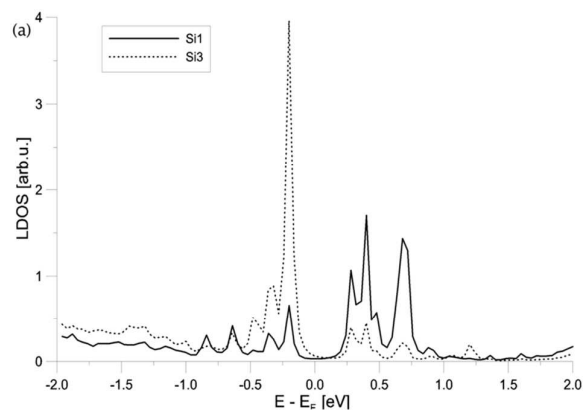
Figure 5. *(Colour online) Local density of states (LDOS) calculated for (a) free ends of chemisorbed dimers **c** and **d** in Fig.2 (atoms Si1 and Si) (b) free ends of dimers **b** and **a** in Fig.2 (atoms Si8 and Si6), (c) ends at the same side of dimer row of two adjacent bare dimers of clean Si(00), and (d) charge density distribution calculated for the state at ~0.2 eV below the Fermi level in LDOS shown in Fig.5a. Isosurface value of 0.003 e/Å³.*
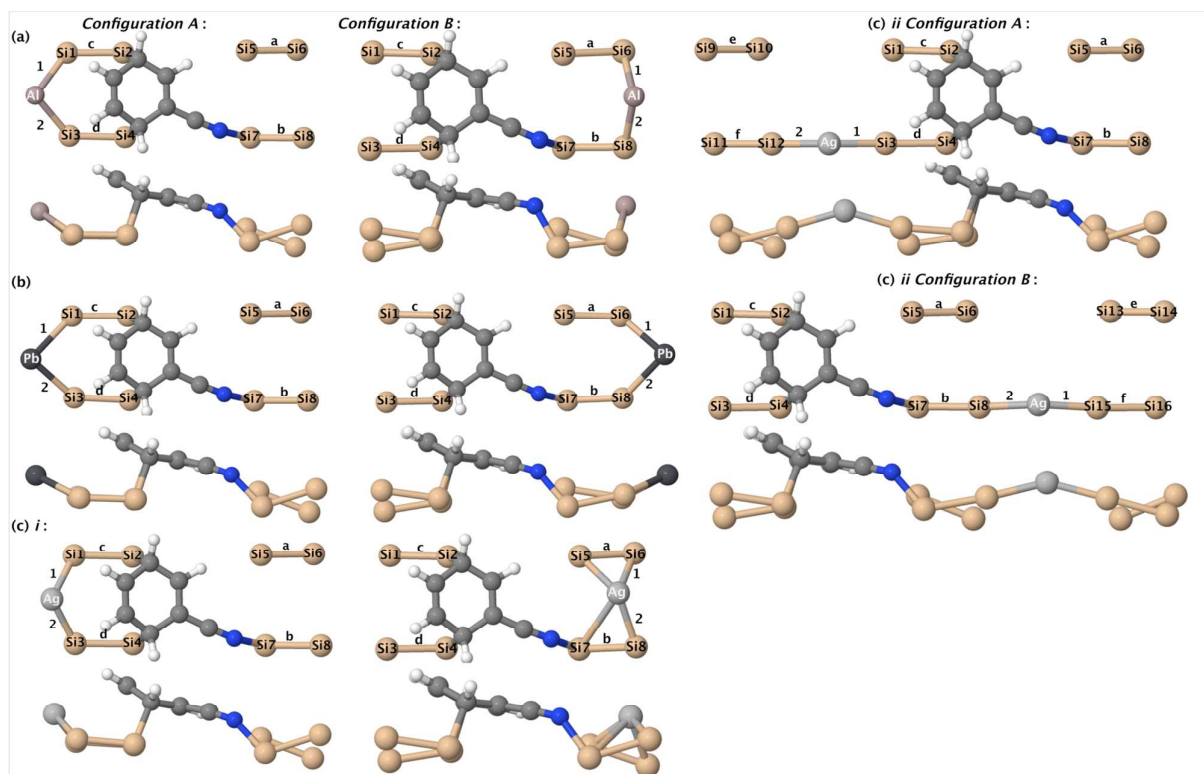
Figure 6. (Colour online) Top and side views of the relaxed structures of the single ad-atoms (a) Al, (b) Pb, and (c) Ag adsorbed on modified, by pre-adsorbed benzonitrile, Si(001). The ad-atoms interact with two dangling bonds on the Si dimers chemisorbed by the phenyl ring (Configuration A), and with a single dangling bond on the Si dimer chemisorbed by the N atom of the nitrile group (Configuration B). In the case of the Ag ad-atom two alternative, stable adsorption structures are shown. Only first layer of Si atoms is shown.
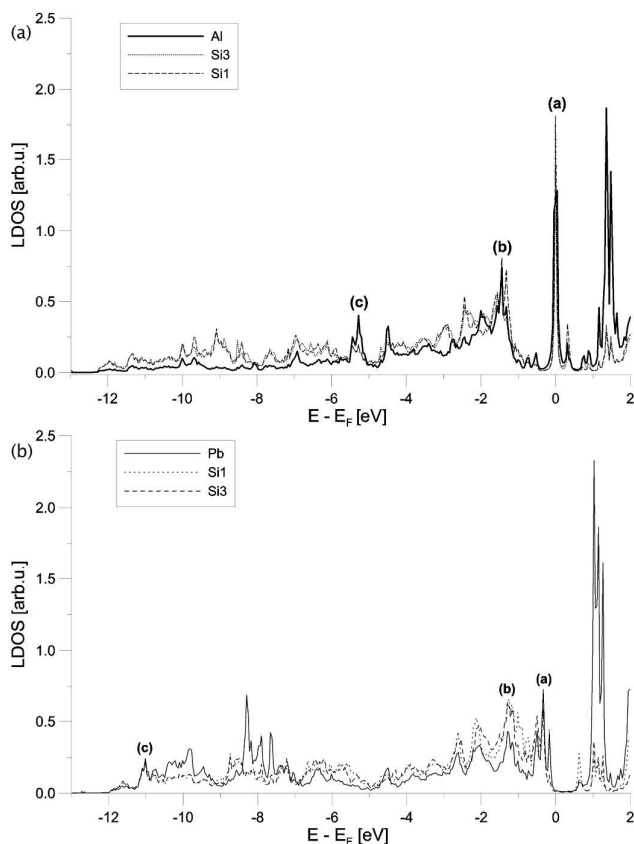
Figure.7. LDOS distributions of the (a) Al and (b) Pb ad-atoms and two Si substrate atoms (S1 and Si3 in Fig.6) interacting directly with the ad-atom - *Configuration **A**.*
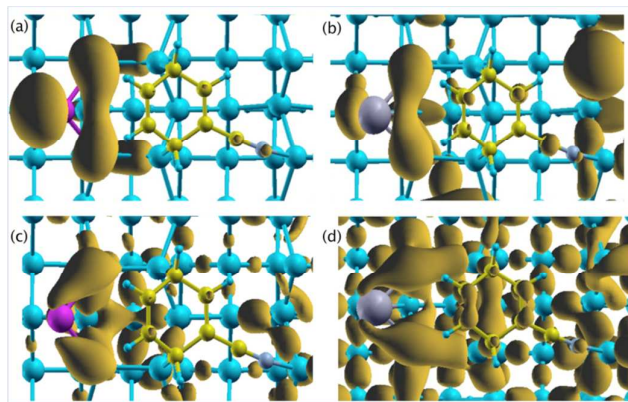
Figure 8. (Colour online) *Configuration **A***: Charge density distributions associated with LDOS features (a) and (b) of Figs.7a for the system with the Al ad-atom – (a,c), and of Fig.7b for the system with the Pb ad-atom – (b,d). Isosurface values: a*) 0.007 e/Å^3*, b) *0.045 e/Å^3*, c) *0.017 e/Å^3*, d) *0.009 e/Å^3.*
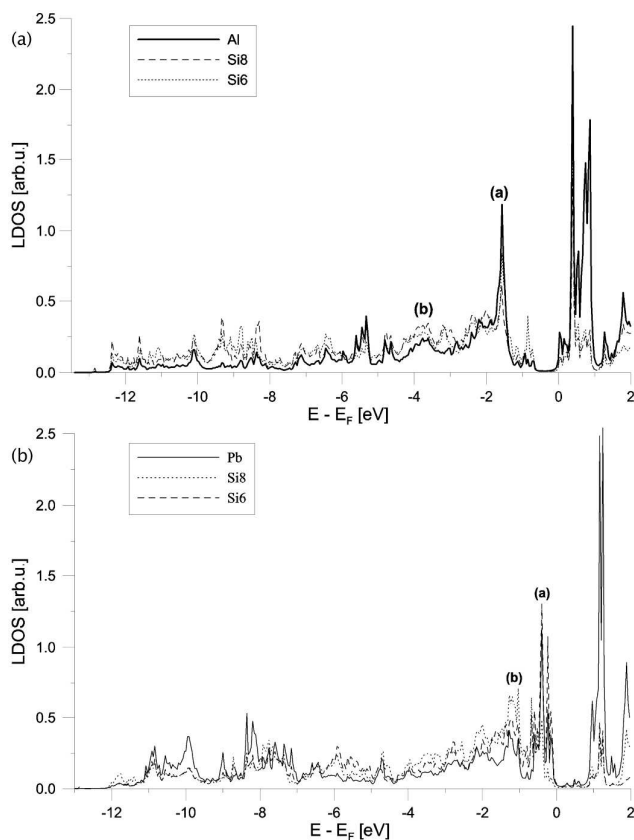
Figure 9. LDOS distributions of the (a) Al and (b) Pb ad-atoms and two Si substrate atoms (S6 and S83 in Fig.6) interacting
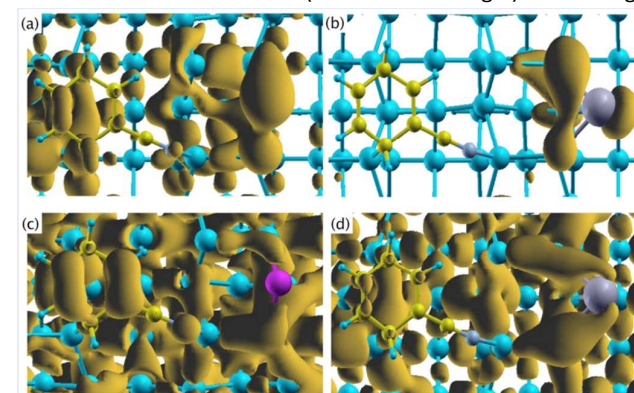
directly with the ad-atom - Configuration **B**.

Figure 10. (Colour online) Configuration **B**: Charge density distributions associated with LDOS features (a) and (b) of Fig.9a for the system with the Al adatom - (a,c), and Fig.9b for the system with the Pb adatom – (b,d) Isosurface values: a) *0.008 e/Å^3*, b) *0.007 e/Å^3*, c) *0.008 e/Å^3*, d) *0.008 e/Å^3.*
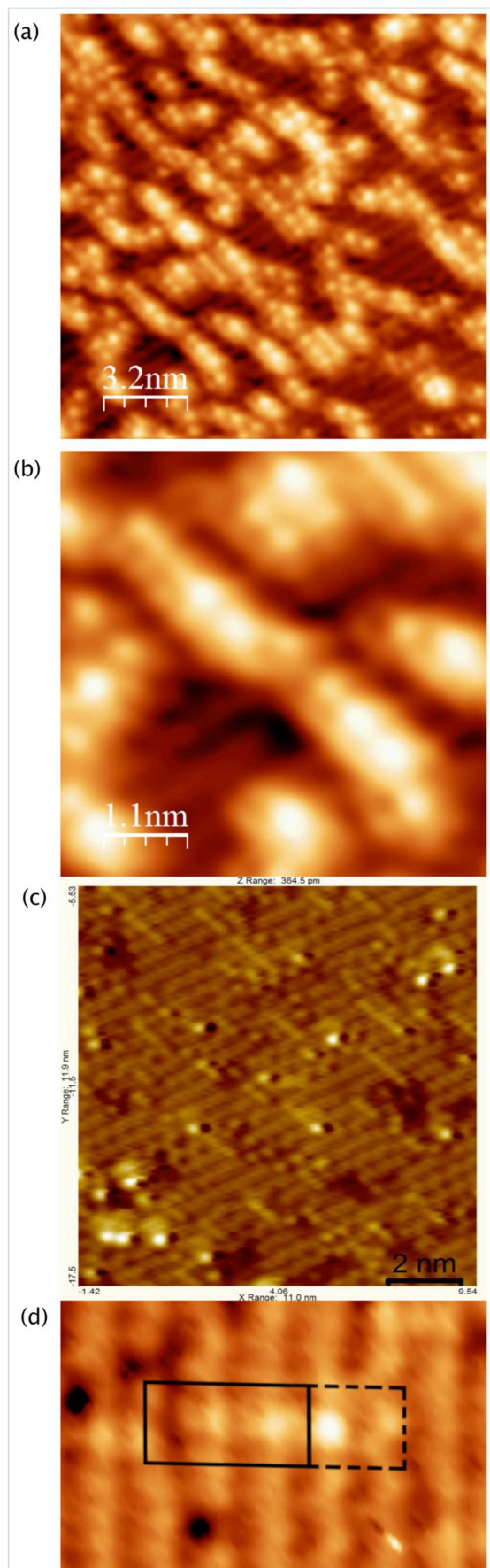
Figure 11. (Colour online) STM images of the formation of the Al chain-like structures pinned to the benzonitrile molecule: (a) unoccupied states (U=2V, I_t = 100pA), (b) zoomed-in on two longer chains extracted from Fig.(a), (c) occupied states (U=-2.2V, I_t = 150pA), (d) zoomed-in on an isolated Al chain pinned to the molecule - occupied states (U=-2.2V, I_t = 150pA). The positions of the molecule and the attached Al chain are indicated by the dashed line and solid line rectangles, respectively.
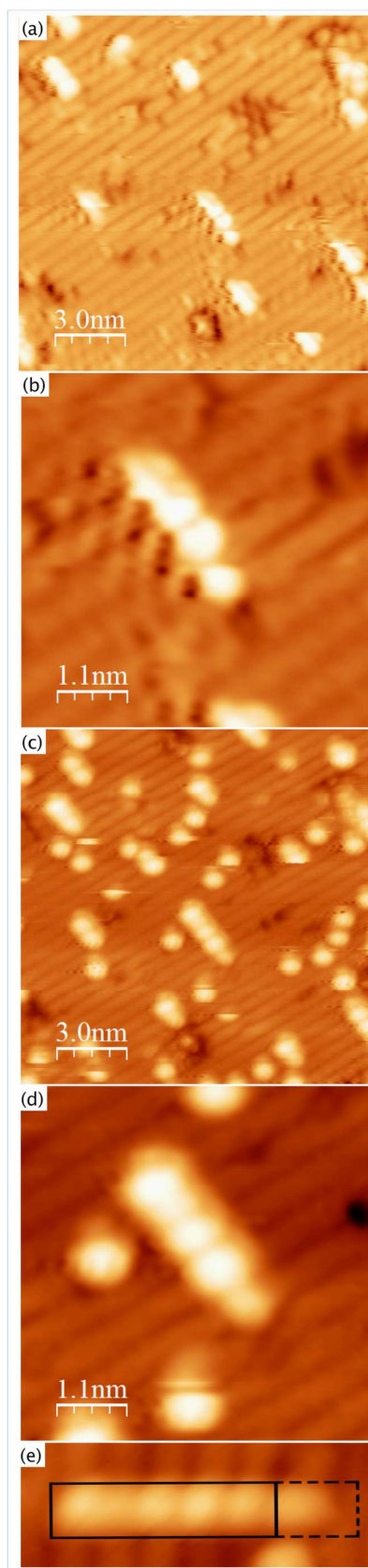
Figure 12. (Colour online) STM images of the Pb chain-like structures pinned to the benzonitrile molecule: (a) occupied states (U=-2V, I_t = 100pA), (b) isolated chain extracted from Fig.(a), (c) unoccupied states (U=2.2V, I_t = 120pA), (d) isolated chain extracted from Fig.(c), (d) an isolated Al chain pinned to the molecule - occupied states (U=-2.2V, I_t = 150pA). (e) isolated Pb chain-like structure hooked at the preadsorbed molecule - unoccupied states (U=2.2 V, I_t = 150 pA). The positions of the molecule and the attached Al chain are indicated by the dashed line and solid line rectangles, respectively.

PhCN/ Si(001)	a	b	c	d	E_{ads}						
	2.35 (21.17)	2.45 (-17.95)	2.40 (-9.41)	2.43 (7.84)	*2.59*						
	1	2	3	4	5	6	7	8	9	10	11
	1.92	1.21	1.40	1.35	1.45	1.48	1.32	1.48	1.49	1.98	1.97

Table I. <u>Upper panel</u>: Calculated adsorption (binding) energy (in eV) of the benzonitrile molecule adsorbed on clean Si(001)-c(4x2) surface (last column). Bond-lengths in Å and the buckling angles in degrees (in brackets) of the bare (a) and chemisorbed (b,c,d) Si dimers of the most stable configuration of Fig.2. A positive buckling angle indicates that the atom on the left is higher that on the right. <u>Lower panel</u>: Inter-atomic distances within the chemisorbed molecule. Symbols (letters and numbers) are the same as in Fig.2.

		1	2	a	b	c	d	e	f	E_{ads}
Config.	Al	2.55	2.52	2.35 (21.19)	2.44 (-17.97)	2.44 (0.11)	2.42 (0.67)	-	-	0.62
A	Pb	2.76	2.71	2.35 (21.41)	2.44 (-17.88)	2.43 (2.24)	2.42 (1.48)	-	-	0.96

	Ag(i)	2.36	2.36	2.35 (21.10)	2.44 (-18.13)	2.43 (3.48)	2.42 (4.98)	-	-	0.58
	Ag(ii)	2.43	2.45	2.35 (21.25)	2.45 (-17.75)	2.38 (-8.48)	2.50 (4.17)	2.34 (22.65)	2.44 (-15.12)	0.64
Config. B	Al	2.46	2.47	2.46 (16.03)	2.42 (-6.98)	2.39 (-9.83)	2.44 (8.63)	-	-	0.12
	Pb	2.71	2.76	2.46 (9.03)	2.44 (-11.79)	2.40 (-9.34)	2.43 (8.00)	-	-	0.21
	Ag(i)	2.57	2.47	2.35 (18.87)	2.42 (-16.99)	2.39 (-9.41)	2.44 (8.47)	-	-	0.30
	Ag(ii)	2.45	2.44	2.34 (21.71)	2.51 (-10.35)	2.39 (-9.54)	2.44 (8.38)	2.34 (-22.76)	2.44 (15.12)	0.47

Table II. Calculated relative adsorption energies (in eV) of the Al, Pb and Ag ad-atoms in Configurations **A** and **B** with respect to their binding energies on clean Si(001)- c(4x2) (last column). The corresponding bond lengths (in Å) and buckling angles of the silicon dimers (in brackets; in °) interacting directly with the ad-atoms are also given (denotation is the same as in Fig.6) A positive buckling angle indicates that the atom on the left is higher that on the right.